MOLECULAR AND CELLULAR BIOLOGY, Apr. 2009, p. 2205–2218 Vol. 29, No. 8
0270-7306/09/$08.00+0 doi:10.1128/MCB.01923-08

Physical Interaction between TBX5 and MEF2C Is Required for Early Heart Development[▽]†

Tushar K. Ghosh,[1] Fei Fei Song,[1] Elizabeth A. Packham,[1] Sarah Buxton,[1] Thelma E. Robinson,[1] Jonathan Ronksley,[1] Tim Self,[2] Andrew J. Bonser,[1] and J. David Brook[1]*

Institute of Genetics, School of Biology,[1] and Institute of Cell Signalling, School of Biomedical Sciences,[2] University of Nottingham, Queen's Medical Centre, Nottingham NG7 2UH, United Kingdom

Received 19 December 2008/Returned for modification 27 January 2009/Accepted 31 January 2009

TBX5 is a transcription factor which plays important roles in the development of the heart and upper limbs. Mutations in this gene produce the inherited disorder Holt-Oram syndrome. Here, we report a physical interaction between TBX5 and MEF2C leading to a synergistic activation of the α-cardiac myosin heavy chain (*MYH6*). Mutants of TBX5, TBX5G80R, and TBX5R279X that produce severe cardiac phenotypes impair the synergy. Using fluorescence resonance energy transfer, we demonstrate the interaction of TBX5 and MEF2C in living cells. We also show that they physically associate through their DNA-binding domains to form a complex on the *MYH6* promoter. Morpholino-mediated knockdowns of Tbx5 and Mef2c in zebrafish suggest that the genetic interaction of these proteins is not only required for *MYH6* expression but also essential for the early stages of heart development and survival. This is the first report of a functional interaction between a T-box protein and a MADS box factor that may be crucial in cardiomyocyte differentiation.

The T-box genes encode transcription factors that play crucial roles in morphogenesis in a wide range of species (36, 40). They share a highly conserved DNA-binding motif, or T domain, of 180 to 200 amino acid residues at their N termini that interact with specific DNA sequences (4, 19, 33). At least 20 members have been identified in humans, and six of these members are linked to developmental disorders (5, 35). Mutations in the gene *TBX5* result in Holt-Oram syndrome, an autosomal-dominant condition in humans featuring severe heart and forelimb abnormalities (2, 23). A direct role for TBX5 in heart and forelimb development has been revealed in animal models (1, 8, 13, 16, 37). The *Tbx5* heterozygous knockout mutant mouse represents a phenocopy of Holt-Oram syndrome (8). Interestingly, although *TBX5* is expressed in the heart, forelimbs, lungs, and eyes, known mutations in *TBX5* affect only the heart and forelimbs. TBX5 specifically interacts with an 8-bp consensus sequence, (A/G)GGTGT(C/G/T)(A/G), to activate the transcription of downstream genes. Thus far, of the few TBX5 targets to have been identified, the cardiac-specific genes *ANF* and *cx*40 are the best characterized (8, 14, 15).

Members of the myocyte enhancer factor 2 (MEF2) family are transcription factors that bind a conserved A/T-rich DNA sequence, (T/C)TA(A/T)$_4$TA(G/A), and transactivate a series of muscle-specific genes (3). In vertebrates, there are four family members, MEF2A, -B, -C, and -D. They share a highly conserved MADS box at their amino termini and an adjacent sequence, known as a MEF2 motif, which together mediate DNA-protein and protein-protein interactions. MEF2C is expressed in heart precursor cells before linear heart tube formation. Targeted disruption of this gene in the mouse results in abnormal looping morphology, and the future right ventricle does not form (24). In *Drosophila*, *Mef2* is expressed throughout the mesoderm following gastrulation. Genetically modified *Drosophila* embryos that lack *Mef2* show a dramatic absence of myosin heavy chain (MHC)-expressing myoblasts and differentiated muscle fibers (6), and Myh6 is downregulated in *Mef2c*$^{-/-}$ mice (24). MEF2s associate with myogenic bHLH proteins, such as MyoD, myogenin, Myf5, and MRF4, and induce muscle cell differentiation. This process is regulated by the interplay of histone deacetylases (25, 27, 41, 44) and calcium calmodulin-dependent protein kinase signaling (25, 26). Recent data also point to interactions between MEF2C and the notch coactivator MALM1 for normal myogenesis (39).

TBX5 is known to interact with the homeodomain protein NKX2.5 (15) and the zinc finger protein GATA4 (12) to coactivate the *ANF* gene and promote cardiomyocyte differentiation. TBX5 also associates with TBX20 (7), TAZ (34), SALL4 (20), and LMP4 (21). Recent studies have shown that the functional cooperation of TBX5 and NKX2.5 on the Id2 promoter is important for the development of the cardiac conduction system (32). Furthermore, MEF2C is known to cooperate with GATA4 to activate *ANF* expression (30). Previously, we identified putative binding sites for TBX5 in the upstream regions of several cardiac-specific genes. Some of these encode structural proteins, including α-MHC and MYH6 (14), suggesting a possible role for TBX5 in their transcriptional regulation. Structural proteins such as MYH6 are the building blocks of cardiomyocytes and are essential for their structure and function. *MYH6*, which is expressed abundantly in the atrium, contains at least 16 putative TBX5-binding sites in its upstream region. Recent studies point to the importance of *MYH6* in heart development and congenital heart disorders (10). In addition, reduced levels of MYH6 also produce an

* Corresponding author. Mailing address: Institute of Genetics, University of Nottingham, Queen's Medical Centre, Nottingham NG7 2UH, United Kingdom. Phone: 44 (0)115 8230314. Fax: 44 (0)115 8230313. E-mail: David.Brook@nottingham.ac.uk.

† Supplemental material for this article may be found at http://mcb.asm.org/.

▽ Published ahead of print on 9 February 2009.

atrial septal defect in morpholino-based knockdown experiments in chicks (10). Other proteins are known to be involved in the regulation of *MYH6*. For example, *MYH6* is synergistically activated by MEF2, the thyroid hormone receptor (22), GATA4, and dHAND (11) and repressed by Yin Yang 1 alone or in conjunction with the Ku protein complex (42, 43).

In view of the roles of TBX5 and MEF2C in the regulation of *MYH6* expression, we examined a potential interaction between these proteins. In this paper, we describe the physical interaction between TBX5 and MEF2C that leads to the synergistic activation of *MYH6*, and we map the respective interaction domains of both proteins. We show that TBX5 and MEF2C interact in vivo and that the double knockdown of Tbx5 and Mef2c in zebrafish produces a significantly increased death rate, severely affecting α-MHC expression and heart development.

MATERIALS AND METHODS

Plasmid construction. Reporter plasmid pGL3-MYH6-I was generated by amplifying a 4.5-kb fragment of the *MYH6* promoter, using the primer pair comprising GCCCTGATTGAAGCCGAGATCCTGA and CTGTCCTCAAAG CTCCAGTTCCTTT, and subsequent cloning into pGL3-basic (Promega). Reporter pGL3-MYH6-IV, which contains a deletion of the region comprising bases −1491 to −1530 from the wild-type reporter pGL3-MYH6-I, was generated using a QuikChange site-directed mutagenesis kit (Stratagene).

In vivo promoter analysis. For in vivo analysis of the MYH6 promoter in zebrafish, we cloned both the wild-type and the mutated promoter sequences into the promoterless reporter vector pEGFP-1 (Clontech). For cloning, the 4.5-kb wild-type and mutated promoter fragments were released from the constructs pGL3-MYH6-I and pGL3-MYH6-IV, respectively, and subcloned into the BglII site of pEGFP-1 to obtain pEGFP-MYH6WT and pEGFP-MYH6MUT. The plasmid DNAs were linearized and injected into one- or two-cell-stage zebrafish embryos (100 to 150 pg per embryo). The injected embryos were analyzed for green fluorescence protein (GFP) expression at 48 hours postfertilization (hpf).

Cell transfection and reporter assays. Rat cardiomyocyte cell line H9c2 and COS7 cells were transfected using Polyfect (Qiagen) according to the manufacturer's protocol. Cells received 1.5 μg of reporter plasmid, 1.0 μg of expression plasmids pcDNA-TBX5 (wild type or mutant) and/or 0.25 μg pcDNA-MEF2C, and 4 ng of plasmid pRL-TK as an internal control to normalize the variation in transfection efficiency between the plates. The total amount of plasmid DNA in each well was adjusted to 3.0 μg by using empty vector pcDNA3.1 as appropriate. Twenty-four hours after transfection, cells were harvested and luciferase activity was measured using a dual luciferase assay kit (Promega). Each transfection experiment was carried out in duplicate and repeated at least three times. Values shown in the histograms are means ± standard deviations. Significance analysis was performed using the Student *t* test.

EMSA. Full-length TBX5-His_6 protein was purified as described previously (14). A His-tagged T domain (His_6-T_d) was generated by cloning the sequence for amino acids 1 to 237 of TBX5 into pET28 (Novagen). Purification of His tag protein was performed with Ni-nitrilotriacetic acid agarose columns (Qiagen). Electrophoretic mobility shift assays (EMSAs) were performed as described previously (14), using a DNA probe corresponding to bases −1491 to −1530 of the *MYH6* promoter. This fragment (designated T1-M-T2) contains two TBX5 sites flanking an A/T-rich site. Probes containing wild-type sequence and mutated transcription factor binding sites were prepared by annealing the oligonucleotides shown in Table 1 to their complements. For supershift assays, we used 2 to 5 μl of polyclonal antibody to either TBX5 (14) or MEF2C (Santa Cruz).

Protein expression constructs. Expression constructs pcDNA-TBX5, pcDNA-TBX5G80R, pcDNA-TBX5G169R, pcDNA-TBX5R237Q, and pcDNA-TBX5 R279X have been described previously (14). A full-length MEF2C expression construct, pcDNA-MEF2C, was generated from IMAGE clone AI879046. The MEF2C clone that we have generated expresses a muscle-specific isoform that lacks the beta peptide in the C-terminal region. Truncated versions of TBX5 and MEF2C were amplified from pcDNA-TBX5 or pcDNA-MEF2C as appropriate and then cloned into pcDNA3.1 (Invitrogen). Maltose-binding protein (MBP)-TBX5 and glutathione *S*-transferase (GST)-MEF2C fusion proteins were generated by cloning the full-length coding sequences of TBX5 and MEF2C into either pMAL-c2X (MBP tag; New England Biolabs) or pGEX-4T-1 (GST tag; Pharmacia). Truncated fusion proteins were constructed in a similar manner. MBP and GST fusion proteins were synthesized in *Escherichia coli* following IPTG (isopropyl-β-D-thiogalactopyranoside) induction and purified on amylose resin (New England Biolabs) and glutathione Sepharose columns (Pharmacia), respectively. Protein quantifications were carried out by a Bradford assay (Bio-Rad). Plasmids pcDNA-MEF2A and pcDNA-MEF2D were kind gifts from Francisco J. Naya (Boston University) and Xiang-Jiao Yang (Montreal University), respectively.

TABLE 1. Oligonucleotides used to generate probes for EMSAs[a]

Probe	Oligonucleotide sequence
T1-M-T2	CAC CTC CAC ACC CTG GAG CTA TAT TGA GAG GTG ACA GTA AAC
T1 mutant	CAC CTC CAG TAC CTG GAG CTA TAT TGA GAG GTG ACA GTA AAC
T2 mutant	CAC CTC CAC ACC CTG GAG CTA TAT TGA GAG ACT ACA GTA AAC
Double mutant	CAC CTC CAG TAC CTG GAG CTA TAT TGA GAG ACT ACA GTA AAC
A/T mutant	CAC CTC CAC ACC CTG GAG CTG CGT TGA GAG GTG ACA GTA AAC

[a] Underlined bases denote mutations.

In vitro coupled transcription/translation. In vitro synthesis of full-length and truncated TBX5 and MEF2C proteins was performed using coupled reticulocyte lysate (Promega) according to the manufacturer's protocol. Briefly, 1.0 to 2.0 μg of template DNA was incubated at 30°C for 90 min in a 50-μl reaction mixture containing [^{35}S]methionine (Amersham). Following incubation, protease inhibitors phenylmethylsulfonyl fluoride (1 mM), leupeptin (1 μg/ml), pepstatin (1 μg/ml), and aprotinin (1 μg/ml) were added to protect samples from proteolysis. Proteins were visualized using sodium dodecyl sulfate-polyacrylamide gel electrophoresis (SDS-PAGE), followed by autoradiography.

In vitro pulldown assays. Full-length or truncated versions of TBX5 proteins were generated as MBP fusion proteins in bacteria following IPTG induction. These fusion proteins were partially purified from bacterial lysates on amylose resin. Their integrity on PAGE gel was checked by Coomassie blue staining of the gel. MBP-TBX5 fusion proteins were immobilized on amylose resin, and GST-MEF2C was immobilized on glutathione Sepharose beads for interaction studies. Equivalent amounts (2 to 5 μg) of immobilized MBP or GST fusion proteins were incubated with ^{35}S-labeled full-length MEF2C or TBX5 (wild type or mutant) in binding buffer (50 mM Tris [pH 7.4], 100 mM NaCl, 0.05% NP-40, 1 mM dithiothreitol [DTT], 10% glycerol, 0.5 mM phenylmethylsulfonyl fluoride, 1 μg/ml aprotinin, 1 μg/ml pepstatin, 1 μg/ml leupeptin, 0.05% bovine serum albumin [BSA]) for 2 h at 4°C. Beads were washed four times with binding buffer without BSA before the bound proteins were released from the beads by boiling with SDS sample buffer. Eluted proteins were subsequently resolved on SDS-PAGE gel, followed by scanning on a Storm PhosphorImager (Amersham Bioscience), and band intensity was quantified using ImageQuant software (Molecular Dynamics).

Immunoprecipitation and Western blot analysis. COS7 cells were transfected with the pcDNA-TBX5, pcDNA-TBX5-Myc, pcDNA-MEF2C or pcDNA-MEF2C-hemagglutinin (HA) expression vector by using Polyfect (Qiagen). Cell extract was prepared after 24 or 48 h by using cell lysis buffer (100 mM NaCl, 20 mM Tris, 10% glycerol, 1% NP-40, 1 mM DTT, and protease inhibitors). For immunoprecipitation, cell extracts were incubated with 30 μl of anti-HA Agarose conjugate (Sigma) overnight at 4°C with gentle shaking. Agarose beads were then washed four times with binding buffer to remove nonspecific interactions. Bound proteins were released from the beads by boiling with sample buffer, resolved on SDS-PAGE gels, and then transferred to polyvinylidene difluoride membranes. Western blot analysis was carried out with either anti-Myc antibody or anti-HA antibody (Sigma), using an ECL Plus kit (Amersham Bioscience).

In vivo interaction studies of TBX5 and MEF2C, using FRET. For fluorescence resonance energy transfer (FRET) studies, we used two well-characterized FRET partners, cyan fluorescence protein (CFP) and yellow fluorescence protein (YFP). The coding sequence of *TBX5* was cloned into the NheI site of the pEYFP-N1 vector and the *MEF2C* coding sequence was cloned into the XhoI and BamHI sites of the pECFP-N1 vector (BD Biosciences) to produce fusion plasmids pTBX5-YFP and pMEF2C-CFP, respectively. In order to generate the pTBX5G80R-YFP construct, we introduced the relevant mutation into the wild-type construct pTBX5-YFP by site-directed mutagenesis using a commercial kit

(Stratagene). The concentration of plasmids pTBX5-YFP and pMEF2C-CFP or pTBX5G80R-YFP and pMEF2C-CFP was optimized for transfection to prevent speckle formation. In control experiments, we transfected COS7 cells with the basic vectors pEYFP-N1 and pECFP-N1. Forty-eight hours after transfection, cells were washed in HEPES-buffered saline and imaged live at 37°C. A Zeiss LSM 510 confocal microscope (Carl Zeiss, Germany) operating with a 25-mW argon laser was used for imaging. The laser was tuned to lines 458 and 514 to excite CFP (458 nm) and YFP (514 nm). With a META spectral detector, emission profiles were generated by scanning emission spectra of MEF2C-CFP and TBX-YFP across a series of wavelengths (462 to 633 nm). FRET was measured using acceptor photobleaching according to the method of Karpova et al. (17). To correct for spectral bleed-through, the images were processed using the linear unmixing emission fingerprinting software for the LSM 510 META apparatus. We selected those cells that show comparable levels of fluorescence for both CFP and YFP. The efficiency of FRET was calculated as a percentage, using the formula $E_F = (I_6 - I_5) \times 100/I_6$, where I_n is the CFP intensity at the nth time point. As the bleach occurred between time points 5 and 6, this formula yields the increase in CFP fluorescence following a YFP bleach normalized by CFP fluorescence after the bleach. As a control, we measured and performed a similar calculation for nonbleached regions of the specimen, using the formula $C_F = (I_6 - I_5) \times 100/I_6$. We analyzed at least 10 cells from each group to derive the significance between the groups. The results are presented as the means ± standard errors of the means, and the significance was calculated using Student's t test.

Microinjection of zebrafish embryos and Western blot analysis. Wild-type zebrafish were kept and staged according to reference 45. Morpholinos for targeting zebrafish *tbx5* (5′-GAAAAGTGTCTTCACTGTCCGCCAT-3′) and *mef2c* (5′-CCTTCCTCTTCCAAAAGTACAGTCC-3′) mRNA were designed and obtained from Gene Tools, LLC. To assess the dose-dependent effects of each morpholino, various dosages of tbx5-MO and mef2c-MO were titrated initially. Wild-type zebrafish embryos at the one- or two-cell stage with an intact chorion were injected with approximately 1.2 to 1.7 nl of stock morpholinos, which ranged from 1 ng/nl to 10 ng/nl in deionized water. The injected embryos were kept at 28.5°C for 2 or 3 days postfertilization. The images of live 3-day-postfertilization zebrafish were captured using a Zeiss Stereo Lumar V12 microscope with a Hamamatsu digital camera.

For Western blot analysis, zebrafish embryos were collected and microinjected with antisense morpholino oligonucleotides for tbx5 (1.2 ng) or mef2c (1.86 ng) or both. At 48 h postinjection, embryos were screened for morphants, collected into Microfuge tubes, washed three times with cold phosphate-buffered saline (PBS), and homogenized five or six times in SDS sample buffer (63 mM Tris buffer [pH 6.8], 10% glycerol, 2% SDS, 1 mM DTT, and protease inhibitors) until uniform in consistency. Following incubation on ice (10 min), the extract was boiled for 5 min and briefly homogenized, followed by centrifugation at 4°C for 10 min at 12,000 rpm. The supernatant was stored at −80°C. The protein concentration of the extract was estimated using a DC protein assay kit (Bio-Rad). For Western blot analysis, 30 μg of total protein from each sample was fractionated on a 4 to 12% Bis-Tris Nu-Page gel (Invitrogen) and electrophoretically transferred to a polyvinylidene difluoride membrane (Invitrogen). The membranes were blocked with 5% nonfat dried milk (Santa Cruz) in Tris-buffered saline containing 0.1% Tween 20 for 2 h at room temperature. The membranes were washed three times (10 min each) in Tris-buffered saline–0.1% Tween 20 and incubated at 4°C overnight with primary antibodies TBX5 (Abnova), Mef2c (Cell Signaling), S46 (Hybridoma Bank), MLC2 (Santa Cruz), cardiac actin (Progen), and α-tubulin (Santa Cruz). Protein detection was carried out with the ECL Plus detection kit (Amersham Bioscience). Protein levels were quantified by scanning band intensities, using ImageQuant 5.2 software.

Immunohistochemistry. Zebrafish embryos (48 hpf) were fixed in 4% paraformaldehyde in PBS overnight at 4°C. The embryos were then washed in PBS-0.1% Tween20 (PBS-T); dehydrated in 25%, 50%, 75%, and 100% methanol; and finally stored overnight in 100% methanol at −20°C. Next day, the embryos were rehydrated by washing them in PBS-T. Embryos were blocked for 4 h at room temperature in blocking solution (5% BSA, 1.0% dimethyl sulfoxide, and 0.1% Tween 20 in PBS), washed briefly in PBS-T, and then incubated overnight at 4°C in a 1:20 dilution of S46 antibody (Developmental Studies Hybridoma Bank) in antibody dilution buffer (3% BSA in PBS-T). The embryos were washed six times at room temperature in PBS-T, followed by 4 h of incubation with secondary antibody (immunoglobulin G-horseradish peroxidase; Sigma) in a dilution of 1:200. After the embryos were washed in PBS-T, diaminobenzidine (Sigma) staining was carried out for color development.

Rescue experiment with zebrafish Myh6. Zebrafish Myh6 is encoded by a single exon. We amplified the entire coding sequence of zebrafish Myh6 by using PCR and cloned it into the pGEM-T vector (Promega). Capped mRNA transcripts were synthesized from the T7 promoter of the NotI-linearized pGEM-Myh6 plasmid DNA by using an mMessage mMachine kit (Ambion). As a control, we used *Xenopus* elongation factor 1α mRNA (Xef-1). Purified *Myh6* or *Xef-1* mRNA (500 pg per embryo) was coinjected with Tbx5 (1.5 ng per embryo) and Mef2c (2.0 ng per embryo) morpholinos into zebrafish embryos. At 48 h postinjection, embryos were screened for heart morphology. The rescue experiment was carried out blind. All the reagents for this experiment were set up by T. Ghosh and coded as X or Y. The actual embryo injection and morphology analysis were carried out by a different person (S. Buxton), without prior knowledge of the reagents, to ensure that the experiment was free from any bias.

RESULTS

TBX5 and MEF2C cooperatively activate transcription of MYH6. Previous studies from our laboratory identified *MYH6* as a target for TBX5 regulation (10, 14). Although TBX5 activates the transcription of at least two other promoters, *ANF* and *CX40*, it shows only weak effects on its own. However, in conjunction with other proteins, TBX5 acts synergistically to produce a severalfold increase in transcription (8, 12, 15). Our promoter analysis suggests that the 4.5-kb upstream region of *MYH6* contains at least 16 putative sites for TBX5, which are clustered into the central and distal intervals. There are also six NKX-binding sites and three GATA sites. Previous work has shown that synergy between neighboring sites is an important feature of cardiac transcriptional regulation (15), but neither NKX- nor GATA-binding sites are in close proximity to the TBX5 sites on the *MYH6* promoter (Fig. 1A). However, within the central region (bases −1491 to −1530), a 40-bp fragment (termed T1-M-T2) containing two TBX5 sites flanking an A/T-rich element, characteristic of a binding site for a cardiac MADS box transcription factor, such as MEF2C, is strongly conserved between human, mouse, hamster, and rabbit (Fig. 1B). In view of the proximity of two TBX5 sites to a putative MEF2C binding site within the *MYH6* upstream region, we performed reporter studies to determine whether the two transcription factors cooperatively activated this gene. The MEF2C expression construct pcDNA-MEF2C was cotransfected with pcDNA-TBX5 and pGL3-MYH6-I in COS7 cells, producing synergistic activation of the myosin reporter gene (Fig. 1C, left). Western blot analysis of the total cell lysate generated from the transfected cells suggest that ectopic expression of either TBX5 or MEF2C does not affect the level of expression of the other protein (Fig. 1C, inset). The TBX5- and MEF2C-mediated synergy was also reproduced in rat H9c2 cells (data not shown). The functional synergy was abolished when we deleted the 40-bp conserved fragment from the wild-type reporter construct, thereby suggesting that the functional interaction of these proteins occurs on this specific region (Fig. 1C, right). This finding is further supported by the in vivo analysis of the 4.5-kb promoter fragment with and without the 40-bp T1-M-T2 section in zebrafish. Full-length and deleted constructs were generated upstream of a promoterless GFP. Deletion of the 40-bp section containing TBX5 and MEF2C sites significantly reduced ($P < 0.01$; wild type versus mutant) the proportion of embryos showing heart fluorescence and the overall level of fluorescence observed (Fig. 1D and E).

Binding site requirement for TBX5 and MEF2C synergy. In order to understand the binding site requirements for TBX5 and MEF2C on the *MYH6* upstream region, we performed gel mobility shift assays. The strongly conserved 40-bp DNA fragment T1-M-T2, corresponding to bases −1491 to −1530 of the

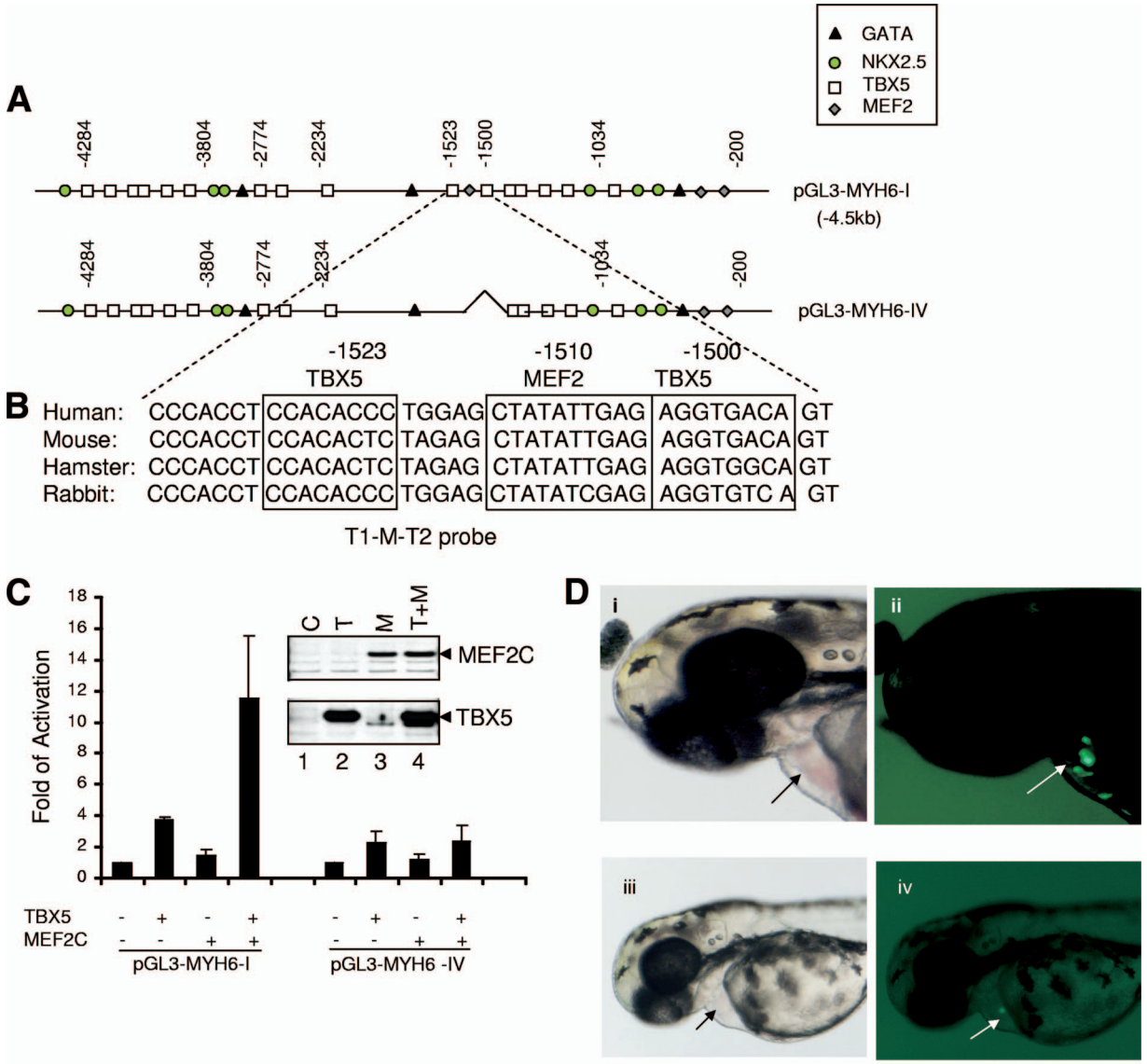

E

Constructs	Total no of GFP Embryos	Heart expression
pEGFP-MYH6WT	163	37%
pEGFP-MYH6MUT	236	16%

FIG. 1. MHC 6 (*MYH6*) is activated by TBX5 and MEF2C. (A) Schematic representation of myosin wild-type and mutant promoter showing the distribution of putative *cis* elements for TBX5, MEF2C, GATA4, and NKX2.5. (B) The sequence of the human *MYH6* promoter region comprising bases −1530 to −1491, which contains two TBX5 sites flanking an MEF2C site, is conserved in mouse, hamster, and rabbit. (C) Histogram showing the synergistic effect of TBX5 and MEF2C on the wild-type *MYH6* promoter and the need for the T1-M-T2 region of pGL3-MYH6-I for TBX5/MEF2C mediated synergy of *MYH6* in COS7 cells. The presence or absence of TBX5 and MEF2C is shown beneath each column. The wild-type reporter construct, pGL3-MYH6-I, is shown on the left and the deleted construct, PGL3-MYH6-IV, on the right. (Inset) Protein levels of TBX5 and MEF2C are shown by Western blot analysis using anti-TBX5 and anti-MEF2C. (D) In vivo promoter analyses of MYH6 in zebrafish. The wild-type (pEGFP-MYH6WT) and 40-bp deletion mutant promoter (pEGFP-MYH6MUT) constructs are injected into one- or two-cell-stage embryos and the 48-hpf embryos screened for GFP expression. Panels i and ii are bright-field and fluorescence images, respectively, of the same embryo injected with the wild-type promoter (lateral view). Panels iii and iv are bright-field and fluorescence images, respectively, of the same embryo injected with the mutant promoter. GFP expression is visible in the heart regions of the embryos (arrow). (E) Table showing the percentages of embryos expressing GFP in the hearts injected with wild-type and mutant constructs.

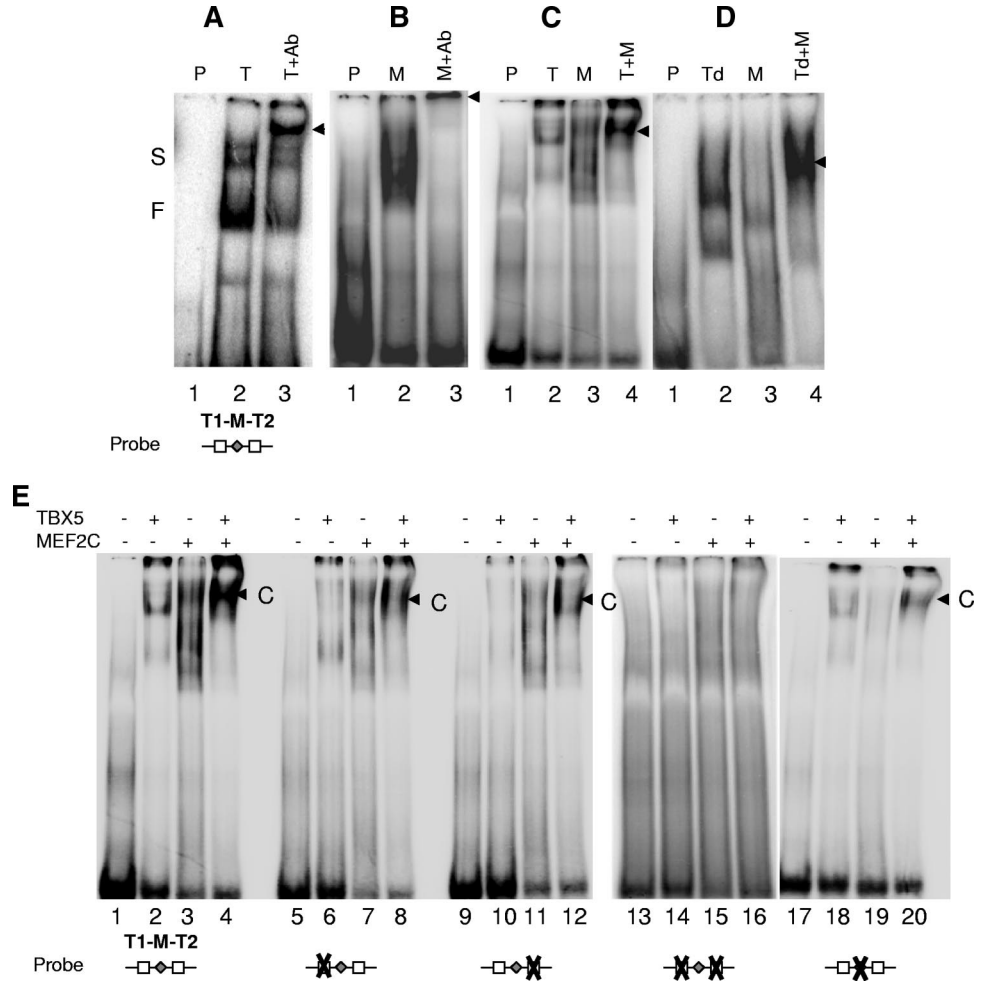

FIG. 2. Binding site requirement for TBX5 and MEF2C synergy on the MYH6 promoter. (A to D) Gel mobility shift assays using T1-M-T2, the 40-bp fragment comprising bases −1491 to −1530 of the MYH6 upstream region (Fig. 1B), as a probe. (A) TBX5 (T) produces fast (F) and slow (S) complexes (lane 2), which can be specifically supershifted using an anti-TBX5 antibody (Ab) (lane 3, arrow). (B) A shifted complex is produced with MEF2C (M) (lane 2) and can be supershifted using an anti-MEF2C antibody (lane 3, arrow). (C) TBX5 (T) and MEF2C (M) together (T+M) form a complex (arrow) on the T1-M-T2 fragment (lane 4). (D) A complex is formed on the T1-M-T2 fragment in the presence of MEF2C (M) and truncated TBX5 containing residues 1 to 237 (Td) (lane 4, arrow). (E) Gel mobility shift assays showing the binding site requirement for complex formation with TBX5 and MEF2C. Wild-type or mutated versions of the T1-M-T2 fragment DNA fragments are shown beneath each set of four lanes. Squares represent TBX5 sites and triangles MEF2C sites. Crosses indicate mutation sites. The arrows indicate the positions of the shifted fragments (C) in lanes 4, 8, 12, and 20, with TBX5 and MEF2C together.

MYH6 upstream interval (Fig. 1B), was used as probe in these studies. Bacterially expressed His-TBX5 produced fast and slow mobility complexes on the T1-M-T2 fragment. These complexes were supershifted by an anti-TBX5-specific antibody (Fig. 2A). A shifted complex was also observed with GST-MEF2C on T1-M-T2, which was supershifted with anti-MEF2C antibody (Fig. 2B). In order to establish whether TBX5 and MEF2C could bind together on the target fragment, we performed EMSAs in the presence of both proteins. Figure 2C shows that MEF2C and TBX5 together form a strong complex, indicating cooperative binding on the DNA target (Fig. 2C, lane 4). A truncated version of TBX5 containing the T domain was sufficient for complex formation with MEF2C on this target (Fig. 2D). In order to determine the binding site requirement for the TBX5-MEF2C interaction, we generated variants of the T1-M-T2 fragment in which the binding sites for TBX5 and MEF2C were mutated in various combinations. Figure 2E shows gel mobility shift assays with wild-type T1-M-T2 and other fragments containing mutant binding sites. The TBX5-MEF2C complex is present in lanes 4, 8, 12, and 20 of Fig. 2E. This shows that mutations in single TBX5 sites (lanes 8 and 12) or in the MEF2C site (lane 20) do not affect complex formation. However, it is affected by mutation in both TBX5 sites (lane 16). These experiments suggest that formation of the complex requires at least one of the TBX5 sites to be intact, whereas the A/T-rich site is not essential.

Association of TBX5 and MEF2C. The synergistic activation of the *MYH6* promoter by TBX5 and MEF2C and the gel mobility shift assay data prompted us to investigate whether there was direct physical association between these proteins by using in vitro pulldown and coimmunoprecipitation assays. Fusion proteins MBP-TBX5 and MBP-LacZ were generated and

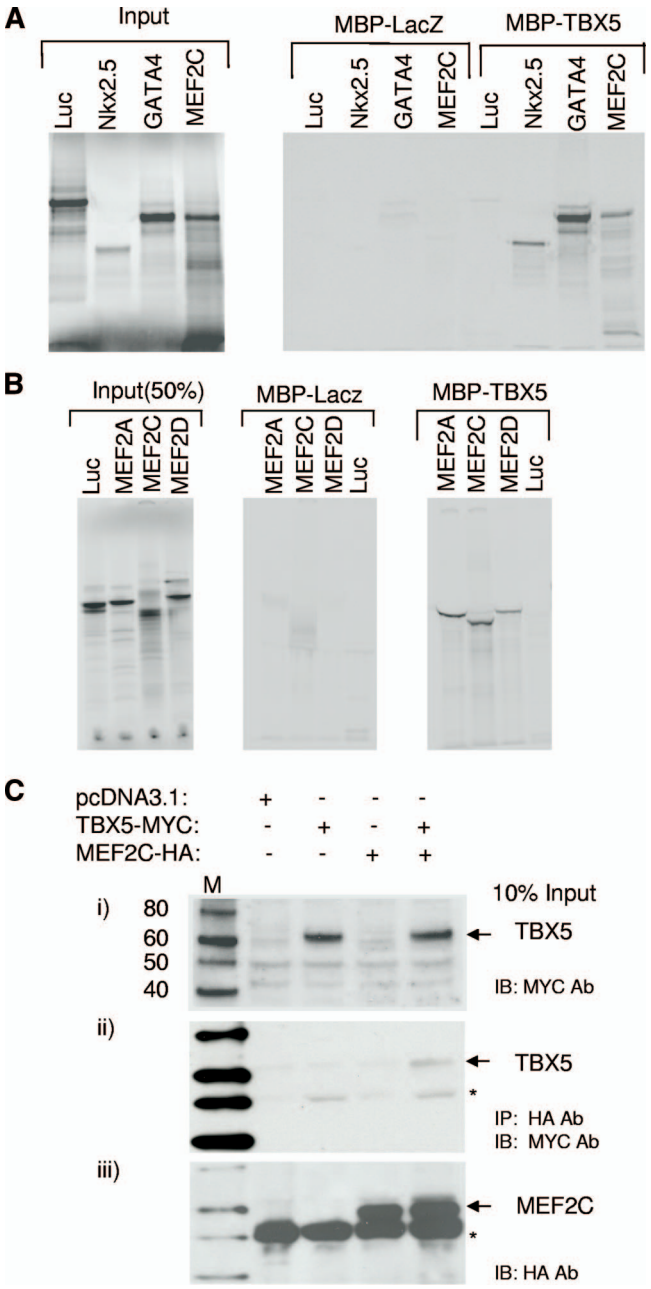

FIG. 3. Physical association of TBX5 and MEF2C. (A) Autoradiographs of pulldown assays showing the extent to which radiolabeled proteins Luciferase (Luc), NKX2.5, GATA4, and MEF2C associate with MBP-TBX5 or MBP-LacZ. The left panel shows a gel containing 50% of the input proteins. The right panel displays the output from the pulldown with MBP-LacZ (control) or MBP-TBX5 and shows the interaction between MBP-TBX5 and MEF2C as well as the interactions between MBP-TBX5 and NKX2.5 or GATA4. The control protein, MBP-LacZ, did not interact with any of these proteins. (B) Similar pulldown assays show that TBX5 also interacts with other MEF2 isoforms, MEF2A and MEF2D. The left panel shows the input gel. The middle and the right panels show the output gels from the pulldown experiments with MBP-LacZ and MBP-TBX5, respectively. (C) Coimmunoprecipitation studies with TBX5-MYC and MEF2C-HA in COS7 cells. The presence or absence of pTBX5-MYC, pMEF2C-HA, or pcDNA3.1 in transfected cells is indicated on the matrix above the Western blots. The lysates from transfected cells were subjected to immunoprecipitation with anti-HA-conjugated agarose beads, and TBX5-MYC was detected using an anti-MYC antibody (Ab). (i) Expression of TBX5-MYC in the input protein. (ii) Copurified TBX5-MYC following HA immunoprecipitation (arrow). (iii) MEF2C protein bound to the beads that copurified the TBX5-MYC protein. Asterisks indicate either nonspecific protein bands (blot ii) or immunoglobulin heavy-chain bands (blot iii). IB indicates the antibody used to probe the relevant blot. IP indicates the antibody used in the immunoprecipitation.

immobilized on amylose resin beads. Following incubation with either in vitro-synthesized, ^{35}S-labeled MEF2C or luciferase proteins, specific interactions were monitored on SDS-polyacrylamide gels. As shown in Fig. 3A, the MBP-TBX5 fusion protein specifically retained the labeled MEF2C protein but not the luciferase control. Under similar conditions, MBP-LacZ failed to interact with MEF2C, indicating that the interaction was specific to TBX5. Figure 3A also illustrates the interaction of TBX5 with NKX2.5 and GATA4 for comparison in parallel assays. Additional pulldown experiments reveal the interaction of MBP-TBX5 with other MEF2 isoforms, such as 2A and 2D (Fig. 3B). Semiquantitative analysis from our pulldown experiments suggests that the affinity of TBX5 for MEF2C is almost two times lower than its affinity for GATA4 and NKX2.5. We also analyzed the affinity of TBX5 for MEF2A and MEF2D. TBX5 shows a similar affinity for MEF2A and MEF2C, but its affinity for MEF2D is almost two-thirds lower.

Coimmunoprecipitation assays were carried out to assess the in vivo association of TBX5 and MEF2C. COS7 cells were transfected with expression constructs pcDNA-TBX5-MYC and pcDNA-MEF2C-HA, either singly or together. At 48 h posttransfection, cell extracts were prepared and immunoprecipitation was carried out using anti-HA-conjugated agarose beads. As shown in Fig. 3C, panel ii, MEF2C-HA could specifically pull down TBX5-MYC in the lysate from the cells coexpressing both proteins, indicating that MEF2C and TBX5 associate in vivo. Our immunoprecipitation studies also suggest that this interaction is particularly salt sensitive (see Fig. S3 in the supplemental material).

Interacting domains of TBX5 and MEF2C. In order to identify the domain of TBX5 that interacts with MEF2C, we generated constructs containing deletions of the N or C termini of TBX5 (Fig. 4A). The truncated versions of TBX5 were expressed as MBP fusion proteins in bacteria and immobilized on amylose beads. Pulldown assays were performed following incubation of the fusion proteins bound to the gel matrix with in vitro-translated, ^{35}S-labeled full-length MEF2C. Whereas N-terminal amino acid residues 1 to 237 of TBX5 interacted with MEF2C, C-terminal residues 238 to 518 failed to do so (Fig. 4A). To fine map the minimal interacting region of the TBX5 T domain, we analyzed further deletion constructs. Deletion of amino acids 1 to 53 did not prevent binding, but further truncation of the T domain from either end resulted in clear reduction of binding activity (Fig. 4B). These results suggest that the DNA-binding domain of TBX5 (residues 54 to 237) is required for mediation of the interaction with MEF2C.

Similarly, we performed pulldown assays to map the domain of MEF2C involved in interaction with TBX5. We generated

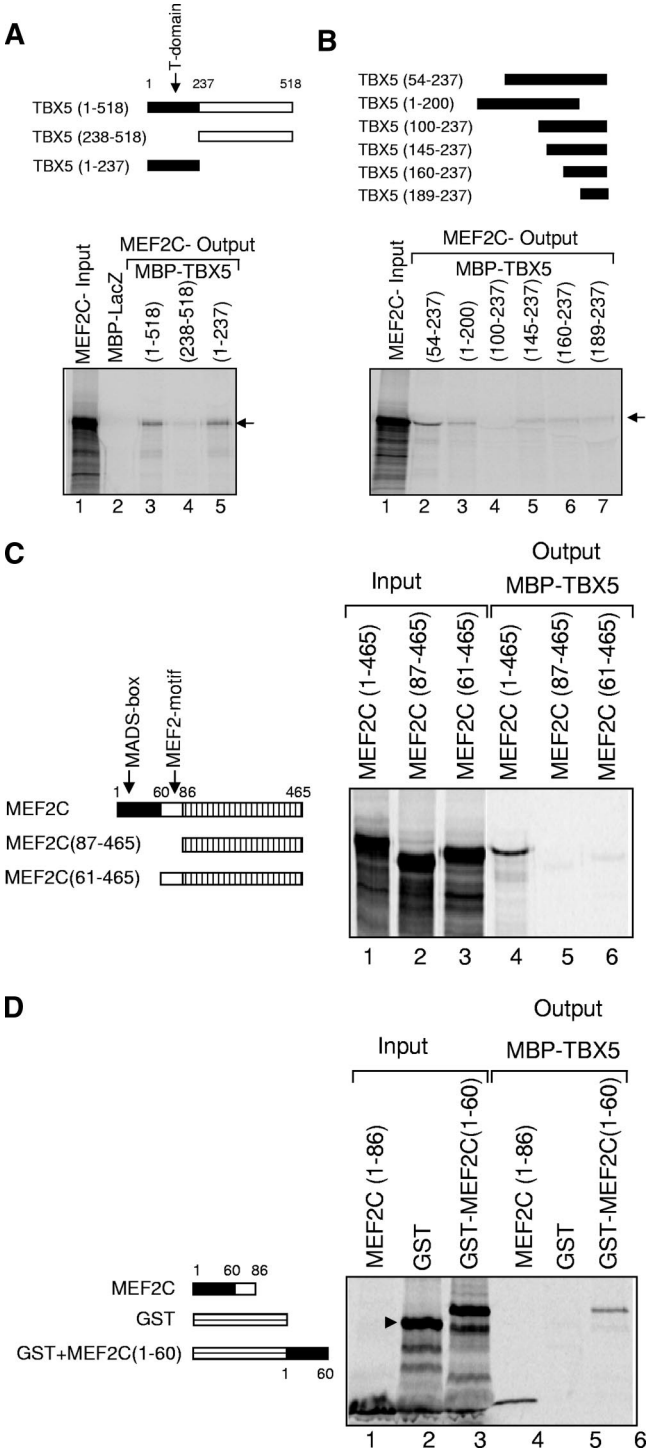

FIG. 4. Mapping the interacting domains of TBX5 and MEF2C. (A) Fragments of TBX5 fused to MBP are shown, with the T domain (residues 1 to 237) in black, alongside an autoradiograph from a pulldown assay. Lane 1, MEF2C input; lanes 2 to 4, MEF2C output with different MBP-tagged TBX5 fragments. (B) Further mapping of residues 1 to 237 of TBX5 by using additional TBX5 deletion constructs fused to MBP. The region of TBX5 present in each case is shown in black. Lane 1, MEF2C input; lanes 2 to 7, MEF2C output following pulldown with the various MBP-tagged fragments of TBX5. (C) Full-length and deletion fragments of MEF2C, tested for binding to full-length TBX5-MBP, are shown schematically alongside an autoradiograph of the pulldown assay. Lanes 1 to 3, MEF2C input proteins; lanes 4 to 6, outputs from these proteins following pulldown with MBP-TBX5. (D) Residues 1 to 60 of MEF2C are essential for binding to TBX5. MEF2C (residues 1 to 86) and the GST-linked MEF2C fragment (residues 1 to 60) are shown schematically, with the MADS box in black, alongside an autoradiograph of the pulldown assay. Lanes 1 to 3, input proteins; lanes 4 to 6, outputs following pulldown with MBP-TBX5.

constructs to produce truncated versions of MEF2C by in vitro-coupled transcription-translation. The truncated proteins were incubated with MBP-TBX5, immobilized on amylose resin, and tested for binding activity. As shown in Fig. 4C, the N-terminal deletion fragments of MEF2C retaining amino acids 87 to 465 and 61 to 465 showed markedly reduced interaction with TBX5. These proteins lack the MADS box motif at the N-terminal end of the protein (residues 1 to 60). To confirm the interaction of the MEF2C MADS box with TBX5, we performed pulldown assays using TBX5 with MEF2C (residues 1 to 86) and TBX5 with a fused peptide containing a small fragment of MEF2C (residues 1 to 60) with a carrier protein GST. MEF2C (residues 1 to 86) and the GST fusion of MEF2C (residues 1 to 60) demonstrated binding to TBX5, whereas GST alone did not interact under similar conditions (Fig. 4D). These data suggest that the TBX5-binding activity of MEF2C lies in the MADS box region between amino acids 1 and 60.

We also examined the effects of various TBX5 mutations in promoter reporter and pulldown assays (see Fig. S1 and associated information in the supplemental material). The TBX5/MEF2C synergy was lost when TBX5R279X, a C-terminal deletion construct, was used. TBX5G80R also showed a significant reduction in synergy with MEF2C, compared to the level for wild-type TBX5, whereas TBX5G169R, TBX5R237Q, and TBX5S252I retained synergistic activation of *MYH6*, but at reduced levels. Furthermore, in reporter assays, TBX5R279X competes in a dominant-negative fashion with wild-type TBX5 for binding to MEF2C and *MYH6* reporter activation (see Fig. S1D in the supplemental material).

TBX5/MEF2C interaction visualized by FRET. To examine whether there is direct interaction of TBX5 and MEF2C under physiological conditions, we performed FRET studies using acceptor photobleaching (Fig. 5). COS7 cells were cotransfected with pTBX5-YFP and pMEF2C-CFP constructs. Following transfection, both proteins were found to colocalize to the nucleus (Fig. 5A and B). Figure S2 in the supplemental material shows images of colocalized pixels only, with significantly increased numbers in the pTBX5-YFP/pMEF2C-CFP-transfected cells. In the colocalized areas, we measured the FRET efficiency from bleached regions (E_F) of at least 10 cells. Control FRET (C_F) from unbleached areas of the same cells was measured. Comparison of these two values provides a clear indication of FRET between TBX5-YFP and MEF2C-CFP ($E_F = 12.53 \pm 2.02$ and $C_F = 0.16 \pm 0.16$) (Fig. 5A to C). FRET was also evident in the control proteins CFP and YFP ($E_F = 5.83 \pm 1.38$ and $C_F = 2.44 \pm 1.17$), possibly due to the nonspecific interactions and/or weak heterodimerization between CFP and YFP molecules (Fig. 5D to F). However, the

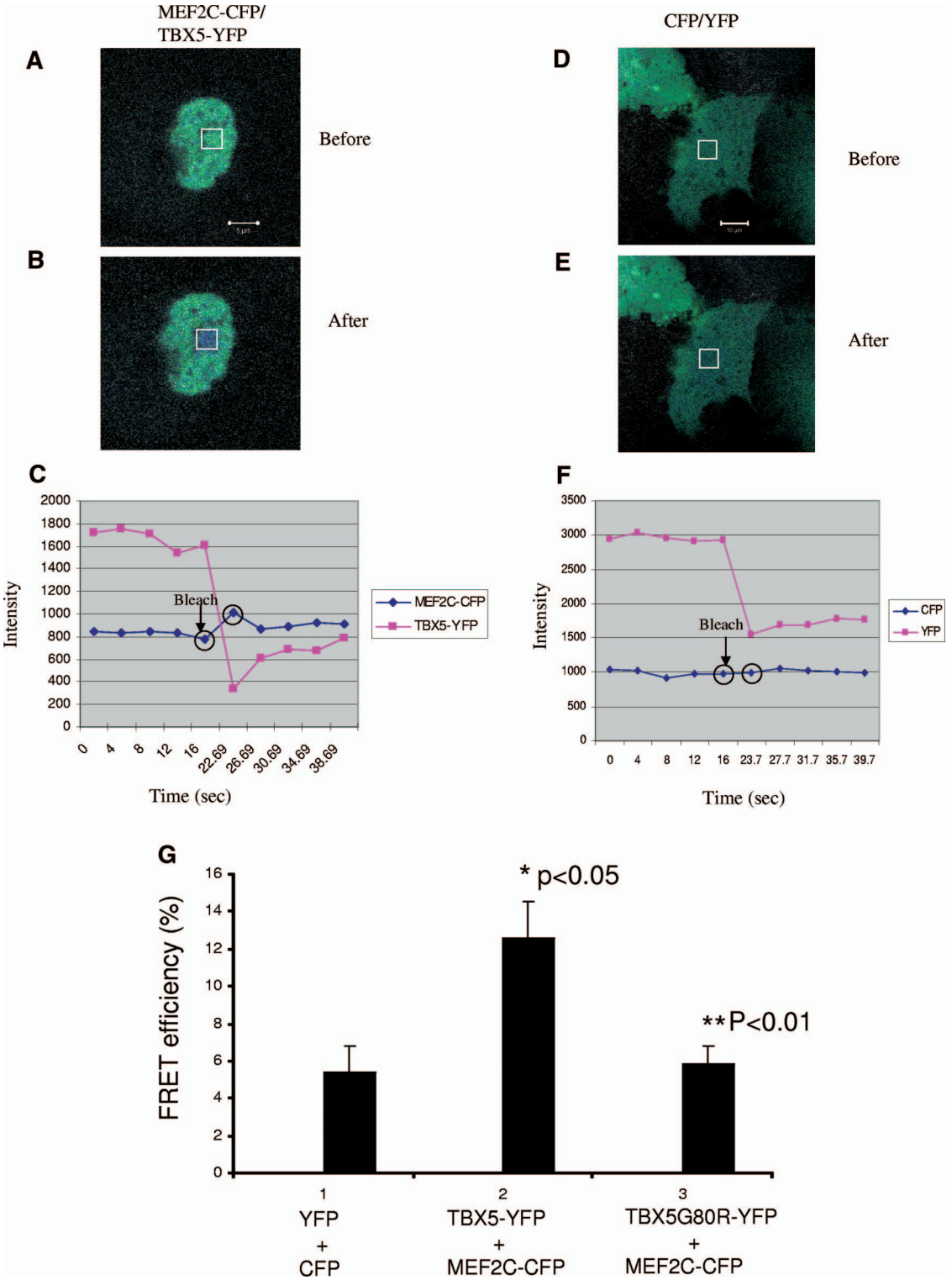

FIG. 5. FRET analysis of TBX5 MEF2C interaction. (A to G) Acceptor photobleaching studies with COS7 cells. Panels A and B are images taken before and after photobleaching in the nucleus of a representative cell cotransfected with pMEF2C-CFP and pTBX5-YFP. Panels D and E are images taken before and after bleaching in a representative cell cotransfected with CFP and YFP plasmid DNA. Panels C and F represent quantification of the fluorescence intensity in the bleached regions of the MEF2C-CFP/TBX5-YFP- and CFP/YFP-expressing cells, respectively. The increase in intensity of CFP fluorescence in the bleached area following photobleaching of YFP in cells cotransfected with pMEF2C-CFP and pTBX5-YFP indicates FRET activity. (G) Histogram showing that FRET activity is significantly higher with TBX5-YFP and MEF2C-CFP than with control proteins CFP and YFP ($P < 0.05$) and that TBX5 mutant protein TBX5G80R-YFP has significantly reduced FRET activity with MEF2C-CFP compared to that with wild-type TBX5-YFP ($P < 0.01$).

TABLE 2. Comparison of death rates in single- and double-knockdown embryos treated with tbx5 and mef2c morpholinos[a]

Expt and morpholino dose	No. of embryos injected	Rate (%) by 48 hpf
Single knockdown		
None (wild type)	2,304	3[b]
5 ng tbx5	140	5[b]
9 ng tbx5	107	14[b]
16.5 ng tbx5	88	11[b]
3 ng mef2c	109	8[b]
7.5 ng mef2c	136	10[b]
8.3 ng mef2c	43	4[b]
Double knockdown		
3 ng each (6 ng total)	30	37[b]
4 ng each (8 ng total)	332	65[b]
5 ng each (10 ng total)	297	79[b]
Single and double knockdown at lower doses		
1.24 ng tbx5	533	21[c]
1.86 ng tbx5 mis	302	1[c]
1.86 ng mef2c	245	6[c]
1.86 ng mef2c mis	233	3[c]
1.24 ng tbx5 + 1.86 ng mef2c	420	52[c]
1.24 ng tbx5 + 1.86 ng mef2c mis	358	19[c]
1.24 ng tbx5 mis + 1.86 ng mef2c	381	21[c]
1.24 ng tbx5 mis + 1.86 ng mef2c mis	285	1[c]

[a] One- or two-cell zebrafish embryos were injected with morpholino, and mortality by 48 hpf was recorded.
[b] Death rate.
[c] Morphant rate.

FRET efficiency was significantly higher with the TBX5-YFP and MEF2C-CFP pairs (Fig. 5A to C) than with the control proteins YFP and CFP (12.53 ± 2.02 versus 5.83 ± 1.38; $P < 0.05$) (Fig. 5D to F). In addition, we also performed FRET studies with a TBX5 mutant, TBX5G80R, as pulldown assays indicate that TBX5G80R mutant protein has a significantly lower affinity for MEF2C than does wild-type TBX5. In FRET assays, the FRET efficiency of TBX5G80R with MEF2C was significantly lower than that for wild-type TBX5 (5.86 ± 0.97 versus 12.53 ± 2.02; $P < 0.01$) (Fig. 5G). Overall, these results suggest that TBX5 directly interacts with MEF2C in a cellular environment.

Effect of Mef2c and Tbx5 knockdown on heart development. To determine the effect of tbx5 and mef2c reduction, we conducted knockdown studies with one- and two-cell zebrafish embryos by using antisense morpholinos against *tbx5* and *mef2c*. Initially, we performed dosage sensitivity studies to optimize the concentration of morpholino employed. Table 2 shows the death rates found for various concentrations of Tbx5-MO and Mef2c-MO when applied singly or in combination. The death rates for embryos following single-morpholino application ranged from 4% to 14%, compared to 3% in controls. In contrast, we observed a strikingly high death rate in embryos in the double-knockdown experiments. Table 2 shows that in the concentration range of 3 ng to 5 ng of each morpholino, the death rate at 48 hpf rose from 37% to 79% in the double knockdowns. This is highly significant, even when the single morpholino with the highest death rate (9 ng Tbx5-MO, in which case 15 of 107 died) (Table 2) is compared to the double knockdown with the lowest death rate (3 ng of Tbx5-MO and 3 ng of Mef2c-MO, in which case 11 out of 30 embryos died) ($P = 0.008$; Fisher's exact test). Because of the very high death rate, we used reduced concentrations (1.24 ng of Tbx5-MO and 1.86 ng of Mef2c-MO) and both were applied simultaneously.

Table 2 shows a comparison of the numbers of morphants observed at 48 hfp in double-knockdown studies using reduced concentrations of targeted and mismatched tbx5 and mef2c morpholinos. The phenotype of the Tbx5 knockdown was as described by others (13), with a stringlike heart, a failure of looping, pericardial edema, and absent or reduced fin buds (Fig. 6). The Mef2c knockdown produced a similar heart phenotype, with looping defects and pericardial edema but normal pectoral fin development. We also conducted experiments with mismatched morpholinos in conjunction with the targeting morpholinos to provide better controls for comparative purposes at lower morpholino concentrations. Tbx5-MO morpholino (1.24 ng) with mismatched Mef2c-MO morpholino (1.86 ng) or Mef2c-Mo (1.86 ng) with mismatched Tbx5-MO (1.24 ng) produced significantly fewer morphants, with generally milder phenotypes, than the double knockdowns, which consistently produced many embryos with a linear unlooped heart. Figure 6 shows the effects of gene knockdown on heart development for a range of zebrafish embryos.

Atrial MHC (myh6) is an in vivo target of Tbx5 and Mef2c. Biochemical and cell transfection studies suggest that TBX5 and MEF2C physically interact and synergistically promote transcription of atrial MHC (*MYH6*). Furthermore, simultaneous treatment with Tbx5-MO and Mef2c-MO morpholinos produced significantly increased levels of death in zebrafish embryos and a more severe phenotype in survivors than treatment with equivalent concentrations of individual morpholinos. Thus, we generated protein extracts from 48-h-postinjection embryos to analyze the levels of putative tbx5 and mef2c targets by Western blot analysis. As shown in Fig. 7, α-MHC (myh6) was significantly reduced following tbx5 and mef2c knockdown, whereas α-cardiac actin and myosin light chain 1a were unaffected. We also compared the effect of the single tbx5 (Fig. 7D, lane 2) or mef2c (Fig. 7D, lane 3) morpholino to that of the double (Fig. 7D, lane 4) morpholinos on myh6 with Western blots. Each single morpholino reduced the level of its target, endogenous tbx5 or mef2c, compared to the level in wild-type embryos. Figure 7D shows that while knockdown of tbx5 or mef2c moderately reduced the level of myh6 (by 16% or 36%, respectively), knockdown of both proteins together reduced the level of myh6 by 68%, suggesting that tbx5 and mef2c cooperatively activate the expression of mhy6 in vivo. In addition, we also performed immunostaining of the tbx5 and mef2c knockdown embryos by using S46, a myh6-specific monoclonal antibody. While both wild-type and mismatched-morpholino-treated embryos show strong myh6 expression in the heart, the antisense morpholinos drastically reduced the myh6 protein in the heart (Fig. 7E).

Myh6 partially rescues the heart phenotype of Tbx5 and Mef2c double-knockdown embryos. Myh6 is significantly downregulated in Tbx5 and Mef2c knockdown embryos. In order to investigate whether the reduced level of Myh6 is at least partly responsible for the heart phenotype in the double-

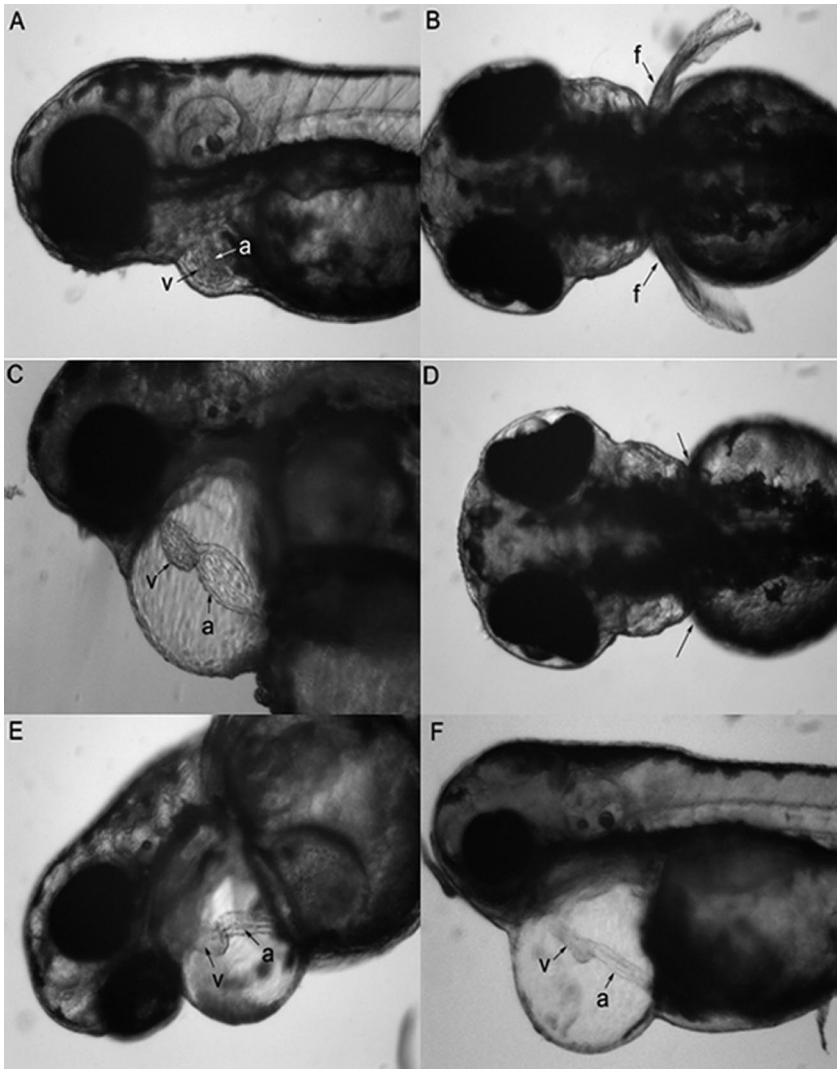

FIG. 6. Knockdown of zebrafish tbx5 or mef2c disrupts looping of the heart tube. (A, B) Wild-type zebrafish showing a tightly looped heart tube and development of the pectoral fins. Zebrafish injected with ~5 ng Tbx5 morpholino show pericardial edema and an unlooped heart tube (C) and no pectoral fin development (arrows indicate absence of fins) (D). (E) Zebrafish treated with ~5 ng Mef2c morpholino also have an unlooped heart tube, but pectoral fin development is unaffected. (F) Embryo following double knockdown with ~1.86 ng of tbx5 and mef2c morpholinos, showing pericardial edema and an unlooped heart tube. a, atrium; v, ventricle; f, fin.

knockdown embryos, we performed rescue experiments with Myh6 RNA. As a control, we used *Xenopus* elongation factor 1α (Xef-1) mRNA. When injected singly, neither Myh6 nor Xef-1 mRNA shows any heart phenotype at the concentration range of 50 to 300 ng. We then coinjected the capped Myh6 mRNA with Tbx5 and Mef2c morpholinos, and in the control group, we coinjected Xef-1 mRNA along with Tbx5 and Mef2c morpholinos. We screened the morphants following both treatments and assigned them to one of four categories (normal, mild, moderate, or severe), based on the severity of heart defects (Fig. 8). Embryo morphology was scored without prior knowledge of the treatment used. Table 3 shows the summary of the rescue experiments. Overall, the data suggest that in comparison to Xef-1, Myh6 RNA significantly ($P < 0.001$; chi-square test) rescued the severity of the heart phenotype in double-knockdown embryos.

DISCUSSION

MHC proteins are the major contractile proteins of the heart. They occur predominantly as two specific isoforms: α-MHC, encoded by *MYH6*, and β-MHC, encoded by *MYH7*. In humans, the two forms are uniformly expressed in the early stage of heart tube formation before finally being restricted predominantly to the atrium (in the case of α-MHC) and the ventricle (in the case β-MHC). *MYH6* and *MYH7* are arranged in tandem on human chromosome 14, separated by 4.5 kb of intergenic sequence. Although the two proteins are highly homologous, their 5′ flanking sequences are quite divergent, indicating different regulatory mechanisms for *MYH6* and *MYH7* transcription (46). Our previous studies identified the presence of several putative binding sites for TBX5 in the *MYH6* upstream region, suggesting that TBX5 might have a direct role

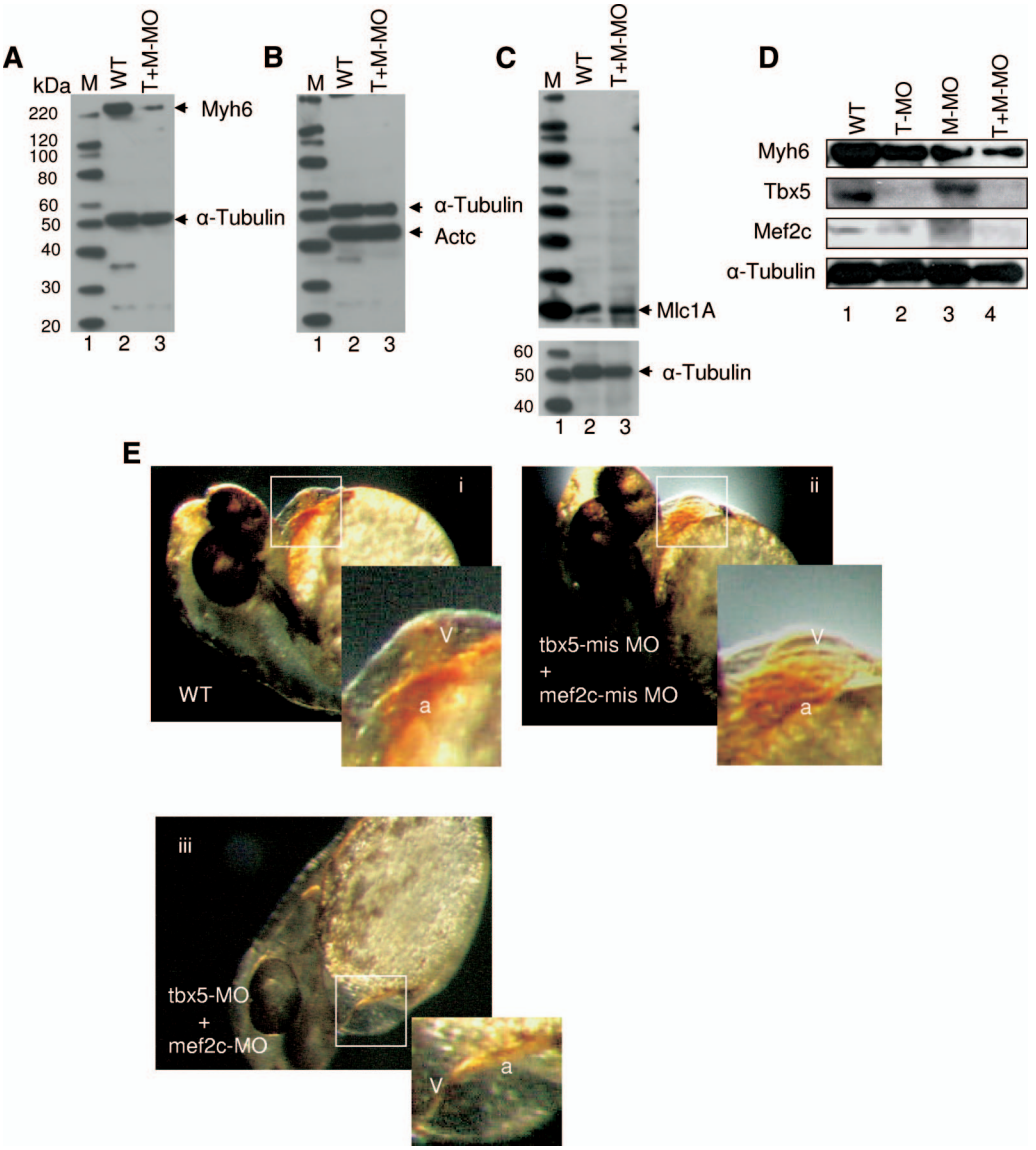

FIG. 7. Effect of tbx5 and mef2c knockdown in zebrafish. Western blots showing the effect of Tbx5 and Mef2c knockdown on the expression levels of anti-MHC (A), anti-cardiac actin (B), and myosin light chain 1a (C). In panels A, B, and C, lane 1 shows the marker (M) (Magic marker; Invitrogen), lane 2 the protein extract from untreated zebrafish embryos (WT), and lane 3 the anti-Tbx5 and anti-Mef2c morpholino-treated samples (T+M-MO). α-Tubulin is shown as a loading control. (D) Western blot analysis showing the effects of Tbx5 and Mef2c single and double knockdown on Myh6 in zebrafish. The blot was probed with antibodies against myh6, tbx5, mef2c, and α-tubulin. Lane 1, wild-type extract (WT); lane 2, tbx5 knockdown extract (T-MO); lane 3, mef2c knockdown extract (M-MO); lane 4, extract from a tbx5-and-mef2c double knockdown (T+M-MO). α-Tubulin is shown as a loading control. (E) Immunostaining of 48-hpf zebrafish embryos showing the expression of Myh6 in the heart (ventral view). (i) Wild-type embryo (WT). (ii) Embryo injected with tbx5 and mef2c mismatch morpholinos (tbx5-Mis MO + mef2c-Mis MO). (iii) Embryo injected with tbx5- and mef2c-targeted morpholinos (tbx5-MO + mef2c-MO), showing a stringlike heart with very little expression of Myh6. The inset shows enlargement of the respective heart regions. a, atrium; v, ventricle.

in the transcriptional regulation of this gene (14). Although TBX5 activates the transcription of at least two other promoters, *ANF* and *CX40*, it shows only weak effects on its own. However, in conjunction with other proteins, TBX5 acts synergistically to produce a severalfold increase in transcription (8, 12, 15). In this study, we report the physical interaction and functional cooperation of TBX5 with MEF2C on the *MYH6* promoter.

The human *MYH6* promoter is not well studied, though one report has shown that it is repressed by the transcription factor Yin Yang 1 (YY1) (43). The 5′ upstream region of the rat α-*MHC* gene contains regulatory elements for transcription factors, such as serum response factor, E box, MEF2, and GATA4 (31), and several of these are present in the human promoter. The proximal region of the rat promoter contains two A/T-rich motifs at positions −219 and −300. The motif at position −300 has little effect (22), whereas the site at position −219, which differs from the MEF2 consensus sequence at a single base (ACTAAAAAAAGG), is indispensable (29) and important for synergy with the thyroid hormone receptor (22).

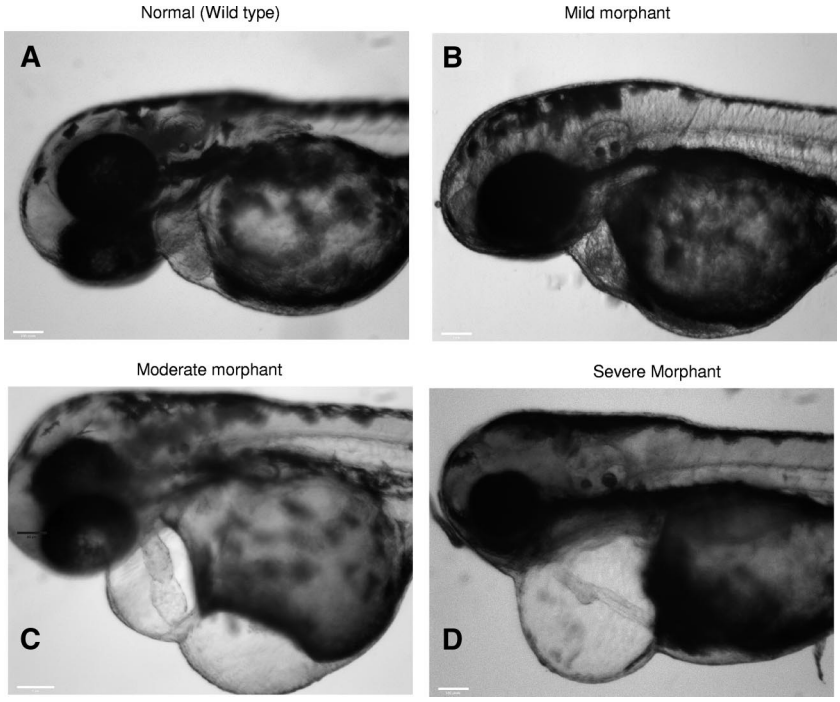

FIG. 8. Heart defects observed in morphants following rescue experiments with Myh6 mRNA in zebrafish. (A) Normal phenotype. Both the atrium and the ventricle are clearly defined (in some cases, it is even possible to observe myocardial and endocardial layers) and tightly packed into a figure eight configuration. (B) Mild phenotype. The atrium and ventricle are clearly distinguishable, but looping is noticeably relaxed and slight pericardial edema is seen. (C) Moderate phenotype. The atrium and ventricle can still be identified but are irregular in shape and/or size. Looping is lost, and pericardial edema is observed. (D) Severe phenotype. Complete malformation is seen, with no defined atrium or ventricle. The heart is stretched to a thin tube. Large pericardial edema is often observed, and the heart rate is notably slower. Many other morphological observations may also be seen (e.g., spinal defects).

We have identified another A/T-rich motif at position −1510 of the human *MYH6* promoter that is flanked by two TBX5 sites (T1-M-T2) and conserved in mouse, hamster, and rabbit. Our promoter search also reveals the presence of six serum response factor sites (positions −4152, −4151, −3723, −2198, −980, and −268) and two SALL sites (positions −3717 and −3025), but neither of the sites is in close proximity to a TBX5 site.

The heterodimerization of various proteins at promoter sites is an effective modulator of gene expression. In some cases, the cognate DNA-binding elements for both protein partners are required for functional cooperation, whereas in other situations, only one site is required to be intact, as the second partner can be recruited to the promoter by physical interaction with the first. The functional cooperation between MEF2 and MyoD (28) and MEF2C and GATA4 (30) requires only one intact cognate site, whereas both DNA-binding sites are required for synergistic activation of *ANF* by TBX5 and NKX2.5 (8) and of rat α-*MHC* by MEF2C and TR (22). In the present study, we have shown that TBX5 and MEF2C form a ternary complex on a promoter fragment containing their cognate sites. The direct recruitment of these two proteins on to the *MYH6* promoter results in the observed synergy. This synergy is abolished when a mutated promoter construct, deleted for the T1-M-T2 region (bases −1491 to −1530) that contains two TBX5 sites and a A/T-rich sites, is used in cotransfection assays. Thus, the assembly of the heterodimer complex in this region of the promoter is obligatory for full transcriptional activation. The EMSAs of the mutated target sites show that the assembly of the TBX5-MEF2C heterodimer complex requires an intact TBX5 site whereas the A/T-rich site is dispensable. We have used FRET to determine whether TBX5 and MEF2C interact in vivo. Studies of transfected cells show that the two proteins interact and that this interaction is significantly reduced with the TBX5G80R mutant. In vitro studies show that the functional cooperation between TBX5 and MEF2C is abrogated by C-terminal deletion of TBX5 and that the mutant TBX5R279X competes with wild-type TBX5 for MEF2C binding, reducing the synergistic effect. Thus, our functional interaction studies with TBX5 mutants and MEF2C suggest that the TBX5 mutant proteins can inhibit transcription of cardiac genes by impairing the synergy with MEF2C. The studies as such provide an important insight into the mechanism of heart defects observed in Holt-Oram syndrome patients.

TABLE 3. Distribution of morphants showing heart phenotypes in the Myh6 rescue experiments

Treatment	No. of embryos showing heart phenotype				Total no. of embryos
	Normal	Mild	Moderate	Severe	
Tbx5-MO + Mef2c-MO + Xef-1 mRNA	31	62	136	172	401
Tbx5-MO + Mef2c-MO + Myh6 mRNA	46	105	150	118	419

Members of the MEF2 family are key regulators of myogenesis. Depending upon local signals, they associate with different groups of repressors or activators and trigger cell proliferation or differentiation. The association mainly occurs through the MADS domain. Our pulldown and immunoprecipitation assays clearly demonstrate that both TBX5 and MEF2C physically associate. Domain mapping studies suggest that the DNA-binding domain (T domain) of TBX5 interacts with the MADS domain of MEF2C. Since the interaction occurs through highly conserved domains, the T box and the MADS box of TBX5 and MEF2C, respectively, it is expected that other members of T-box family, such as TBX2, -3, and -20, will also interact with MEF2C. Similarly, it is expected that other MEF2 members, by virtue of their shared MADS box domain, will interact with TBX5. Indeed, our pulldown experiments suggest that two other MEF2 members, MEF2A and MEF2D, also interact with TBX5. The T domain of TBX5 also interacts with NKX2.5 (15) and GATA4 (unpublished observation). Also, a group of activators, such as MyoD (18, 28), p300 (38), thyroid hormone receptor (22), GATA4 (30), and the steroid receptor GRIP-1 (9), interacts with MEF2 through the MADS/MEF2 domain. Thus, the domains through which TBX5 and MEF2C interact are also bound by numerous other transcriptional modulators.

To investigate further the TBX5 MEF2C interaction in vivo, we performed morpholino knockdown studies with zebrafish. The Tbx5-MO knockdown produced a phenotype similar to that described for the zebrafish *heartstrings* mutant, which has a premature stop at amino acid 316 of Tbx5. In this mutant, the fin buds are absent or reduced. The heart appears normal and functions during the early heart tube stage, but subsequently, it fails to loop and there is a deterioration of the atria and ventricles (13). The Mef2c knockdown produced a similar phenotype, with obvious failure of cardiac looping and pericardial edema but, in this case, no disruption of fin bud development. The most striking effect was observed with the Tbx5-MO-and-Mef2c-MO double knockdown, which proved lethal at relatively low concentrations of morpholino, compared to the effect observed with each of the single morpholinos at equivalent concentrations. At present, it is difficult to determine the exact cause of death, but one possible mechanism in the double knockdowns might be structural and functional defects in the heart, as our double-knockdown embryos show a severe heart phenotype. The markedly increased sensitivity to combined reduction of Tbx5 and Mef2c indicates possible synergistic effects of these proteins on downstream targets. In view of the FRET data and the in vitro data suggesting interaction between TBX5 and MEF2C and their activation of the MYH6 promoter, we examined the expression of the zebrafish myh6 protein in the double knockdowns. Western blots show that the level of myh6 is significantly reduced in the double-knockdown embryos, whereas actc and mlc1a are not altered. Myh6 mRNA partially rescues the heart phenotype in Tbx5 and Mef2c double-knockdown embryos, thereby suggesting a possible regulatory network involving these three genes in heart development and disorders. The coexpression of tbx5, mef2c, and myh6 prior to and during the formation of the linear heart tube is consistent with the involvement and interaction of these three proteins at the earliest stages of heart development. Taken together, these data suggest that tbx5 and mef2c interact to affect α-MHC expression.

The data presented here demonstrate that TBX5 physically associates with MEF2C in vitro and in vivo and cooperatively activates transcription from the *MYH6* promoter. Similar interactions of TBX5 with the homeodomain protein NKX2.5 (15) or the zinc finger protein GATA4 (12) also result in synergistic activation of genes involved in cardiac differentiation. Mutations in the *TBX5*, *NKX2.5*, or *GATA4* human gene result in a common etiology, cardiac septation defects, possibly mediated via a common set of target genes in the septation pathway. The functional cooperation of TBX5 and MEF2C links MEF2C to the higher-order protein complex regulating heart development. As such, it represents a further candidate gene for mutational screening in familial and sporadic cases of congenital heart disease, which provides novel insights into the molecular genetic control of cardiac development.

ACKNOWLEDGMENTS

This work was funded by the British Heart Foundation and the Wellcome Trust.

REFERENCES

1. **Agarwal, P., J. N. Wylie, J. Galceran, O. Arkhitko, C. Li, C. Deng, R. Grosschedl, and B. G. Bruneau.** 2003. Tbx5 is essential for forelimb bud initiation following patterning of the limb field in the mouse embryo. Development **130:**623–633.
2. **Basson, C. T., D. R. Bachinsky, R. C. Lin, T. Levi, J. A. Elkins, J. Soults, D. Grayzel, E. Kroumpouzou, T. A. Traill, J. Leblanc-Straceski, B. Renault, R. Kucherlapati, J. G. Seidman, and C. E. Seidman.** 1997. Mutations in human *TBX5* cause limb and cardiac malformation in Holt-Oram syndrome. Nat. Genet. **15:**30–35.
3. **Black, B. L., and E. N. Olson.** 1998. Transcriptional control of muscle development by myocyte enhancer factor-2 (MEF2) proteins. Annu. Rev. Cell Dev. Biol. **14:**167–196.
4. **Bollag, R. J., Z. Siegfried, J. A. Cebra-Thomas, N. Garvey, E. M. Davison, and L. M. Silver.** 1994. An ancient family of embryonically expressed mouse genes sharing a conserved protein motif with the T locus. Nat. Genet. **7:**383–389.
5. **Bongers, E. M., P. H. Duijf, S. E. van Beersum, J. Schoots, A. Van Kampen, A. Burckhardt, B. C. Hamel, F. Losan, L. H. Hoefsloot, H. G. Yntema, N. V. Knoers, and H. van Bokhoven.** 2004. Mutations in the human TBX4 gene cause small patella syndrome. Am. J. Hum. Genet. **74:**1239–1248.
6. **Bour, B. A., M. A. Obrien, W. L. Lockwood, E. S. Goldstein, R. Bodmer, P. H. Taghert, S. M. Abmayr, and H. T. Nguyen.** 1995. Drosophila MEF2, a transcription factor that is essential for myogenesis. Genes Dev. **9:**730–741.
7. **Brown, D. D., S. N. Martz, O. Binder, S. C. Goetz, B. M. Price, J. C. Smith, and F. L. Conlon.** 2005. Tbx5 and Tbx20 act synergistically to control vertebrate heart morphogenesis. Development **132:**553–563.
8. **Bruneau, B. G., G. Nemer, J. P. Schmitt, F. Charron, L. Robitaille, S. Caron, D. A. Conner, M. Gessler, M. Nemer, C. E. Seidman, and J. G. Seidman.** 2001. A murine model of Holt-Oram syndrome defines roles of the T-box transcription factor Tbx5 in cardiogenesis and disease. Cell **106:**709–721.
9. **Chen, S. L., D. H. Dowhan, B. M. Hosking, and G. E. Muscat.** 2000. The steroid receptor coactivator, GRIP-1, is necessary for MEF-2C-dependent gene expression and skeletal muscle differentiation. Genes Dev. **14:**1209–1228.
10. **Ching, Y. H., T. K. Ghosh, S. J. Cross, E. A. Packham, L. Honeyman, S. Loughna, T. E. Robinson, A. M. Dearlove, G. Ribas, A. J. Bonser, N. R. Thomas, A. J. Scotter, L. S. Caves, G. P. Tyrrell, R. A. Newbury-Ecob, A. Munnich, D. Bonnet, and J. D. Brook.** 2005. Mutation in myosin heavy chain 6 causes atrial septal defect. Nat. Genet. **37:**423–428.
11. **Dai, Y. S., P. Cserjesi, B. E. Markham, and J. D. Molkentin.** 2002. The transcription factors GATA4 and dHAND physically interact to synergistically activate cardiac gene expression through a p300-dependent mechanism. J. Biol. Chem. **277:**24390–24398.
12. **Garg, V., I. S. Kathiriya, R. Barnes, M. K. Schluterman, I. N. King, C. A. Butler, C. R. Rothrock, R. S. Eapen, K. Hirayama-Yamada, K. Joo, R. Matsuoka, J. C. Cohen, and D. Srivastava.** 2003. GATA4 mutations cause human congenital heart defects and reveal an interaction with TBX5. Nature **424:**443–447.
13. **Garrity, D. M., S. Childs, and M. C. Fishman.** 2002. The heartstrings mutation in zebrafish causes heart/fin Tbx5 deficiency syndrome. Development **129:**4635–4645.

14. **Ghosh, T. K., E. A. Packham, A. J. Bonser, T. E. Robinson, S. J. Cross, and J. D. Brook.** 2001. Characterization of the TBX5 binding site and analysis of mutations that cause Holt-Oram syndrome. Hum. Mol. Genet. **10:**1983–1994.
15. **Hiroi, Y., S. Kudoh, K. Monzen, Y. Ikeda, Y. Yazaki, R. Nagai, and I. Komuro.** 2001. Tbx5 associates with Nkx2-5 and synergistically promotes cardiomyocyte differentiation. Nat. Genet. **28:**276–280.
16. **Horb, M. E., and G. H. Thomsen.** 1999. Tbx5 is essential for heart development. Development **126:**1739–1751.
17. **Karpova, T. S., C. T. Baumann, L. He, X. Wu, A. Grammer, P. Lipsky, G. L. Hager, and J. G. McNally.** 2003. Fluorescence resonance energy transfer from cyan to yellow fluorescent protein detected by acceptor photobleaching using confocal microscopy and a single laser. J. Microsc. **209:**56–70.
18. **Kaushal, S., J. W. Schneider, B. Nadal-Ginard, and V. Mahdavi.** 1994. Activation of the myogenic lineage by MEF2A, a factor that induces and cooperates with MyoD. Science **266:**1236–1240.
19. **Kispert, A., and B. G. Hermann.** 1993. The Brachyury gene encodes a novel DNA binding protein. EMBO J. **12:**4898–4899.
20. **Koshiba-Takeuchi, K., J. K. Takeuchi, E. P. Arruda, I. S. Kathiriya, R. Mo, C. C. Hui, D. Srivastava, and B. G. Bruneau.** 2006. Cooperative and antagonistic interactions between Sall4 and Tbx5 pattern the mouse limb and heart. Nat. Genet. **38:**175–183.
21. **Krause, A., W. Zacharias, T. Camarata, B. Linkhart, E. Law, A. Lischke, E. Miljan, and H. G. Simon.** 2004. Tbx5 and Tbx4 transcription factors interact with a new chicken PDZ-LIM protein in limb and heart development. Dev. Biol. **273:**106–120.
22. **Lee, Y., B. Nadal-Ginard, V. Mahdavi, and S. Izumo.** 1997. Myocyte-specific enhancer factor 2 and thyroid hormone receptor associate and synergistically activate the alpha-cardiac myosin heavy-chain gene. Mol. Cell. Biol. **17:**2745–2755.
23. **Li, Q. Y., R. A. Newbury-Ecob, J. A. Terrett, D. I. Wilson, A. R. Curtis, C. H. Yi, T. Gebuhr, P. J. Bullen, S. C. Robson, T. Strachan, D. Bonnet, S. Lyonnet, I. D. Young, J. A. Raeburn, A. J. Buckler, D. J. Law, and J. D. Brook.** 1997. Holt-Oram syndrome is caused by mutations in TBX5, a member of the Brachyury (T) gene family. Nat. Genet. **15:**21–29.
24. **Lin, Q., J. Schwarz, C. Bucana, and E. N. Olson.** 1997. Control of mouse cardiac morphogenesis and myogenesis by transcription factor MEF2C. Science **276:**1404–1407.
25. **Lu, J., T. A. McKinsey, C. L. Zhang, and E. N. Olson.** 2000. Regulation of skeletal myogenesis by association of the MEF2 transcription factor with class II histone deacetylases. Mol. Cell **6:**233–244.
26. **McKinsey, T. A., C. L. Zhang, J. Lu, and E. N. Olson.** 2000. Signal-dependent nuclear export of a histone deacetylase regulates muscle differentiation. Nature **408:**106–111.
27. **Miska, E. A., C. Karlsson, E. Langley, S. J. Nielsen, J. Pines, and T. Kouzarides.** 1999. HDAC4 deacetylase associates with and represses the MEF2 transcription factor. EMBO J. **18:**5099–5107.
28. **Molkentin, J. D., B. L. Black, J. F. Martin, and E. N. Olson.** 1995. Cooperative activation of muscle gene expression by MEF2 and myogenic bHLH proteins. Cell **83:**1125–1136.
29. **Molkentin, J. D., and B. E. Markham.** 1993. Myocyte-specific enhancer-binding factor (MEF-2) regulates alpha-cardiac myosin heavy chain gene expression in vitro and in vivo. J. Biol. Chem. **268:**19512–19520.
30. **Morin, S., F. Charron, L. Robitaille, and M. Nemer.** 2000. GATA-dependent recruitment of MEF2 proteins to target promoters. EMBO J. **19:**2046–2055.
31. **Morkin, E.** 2000. Control of cardiac myosin heavy chain gene expression. Microsc. Res. Tech. **50:**522–531.
32. **Moskowitz, I. P., J. B. Kim, M. L. Moore, C. M. Wolf, M. A. Peterson, J. Shendure, M. A. Nobrega, Y. Yokota, C. Berul, S. Izumo, J. G. Seidman, and C. E. Seidman.** 2007. A molecular pathway including Id2, Tbx5, and Nkx2-5 required for cardiac conduction system development. Cell **129:**1365–1376.
33. **Muller, C. W., and B. G. Herrmann.** 1997. Crystallographic structure of the T domain-DNA complex of the Brachyury transcription factor. Nature **389:**884–888.
34. **Murakami, M., M. Nakagawa, E. N. Olson, and O. Nakagawa.** 2005. A WW domain protein TAZ is a critical coactivator for TBX5, a transcription factor implicated in Holt-Oram syndrome. Proc. Natl. Acad. Sci. USA **102:**18034–18039.
35. **Packham, E. A., and J. D. Brook.** 2003. T-box genes in human disorders. Hum. Mol. Genet. **12**(Spec. No. 1)**:**R37–R44.
36. **Papaioannou, V. E.** 2001. T-box genes in development: from hydra to humans. Int. Rev. Cytol. **207:**1–70.
37. **Rallis, C., B. G. Bruneau, J. Del Buono, C. E. Seidman, J. G. Seidman, S. Nissim, C. J. Tabin, and M. P. Logan.** 2003. Tbx5 is required for forelimb bud formation and continued outgrowth. Development **130:**2741–2751.
38. **Sartorelli, V., J. Huang, Y. Hamamori, and L. Kedes.** 1997. Molecular mechanisms of myogenic coactivation by p300: direct interaction with the activation domain of MyoD and with the MADS box of MEF2C. Mol. Cell. Biol. **17:**1010–1026.
39. **Shen, H., A. S. McElhinny, Y. Cao, P. Gao, J. Liu, R. Bronson, J. D. Griffin, and L. Wu.** 2006. The Notch coactivator, MAML1, functions as a novel coactivator for MEF2C-mediated transcription and is required for normal myogenesis. Genes Dev. **20:**675–688.
40. **Smith, J.** 1999. T-box genes: what they do and how they do it. Trends Genet. **15:**154–158.
41. **Sparrow, D. B., E. A. Miska, E. Langley, S. Reynaud-Deonauth, S. Kotecha, N. Towers, G. Spohr, T. Kouzarides, and T. J. Mohun.** 1999. MEF-2 function is modified by a novel co-repressor, MITR. EMBO J. **18:**5085–5098.
42. **Sucharov, C. C., S. M. Helmke, S. J. Langer, M. B. Perryman, M. Bristow, and L. Leinwand.** 2004. The Ku protein complex interacts with YY1, is up-regulated in human heart failure, and represses α myosin heavy-chain gene expression. Mol. Cell. Biol. **24:**8705–8715.
43. **Sucharov, C. C., P. Mariner, C. Long, M. Bristow, and L. Leinwand.** 2003. Yin Yang 1 is increased in human heart failure and represses the activity of the human alpha-myosin heavy chain promoter. J. Biol. Chem. **278:**31233–31239.
44. **Wang, A. H., N. R. Bertos, M. Vezmar, N. Pelletier, M. Crosato, H. H. Heng, J. Th'ng, J. Han, and X. J. Yang.** 1999. HDAC4, a human histone deacetylase related to yeast HDA1, is a transcriptional corepressor. Mol. Cell. Biol. **19:**7816–7827.
45. **Westerfield, M.** 1993. The zebrafish book: a guide for the laboratory use of zebrafish (Brachydanio rerio), 4th ed. University of Oregon Press, Eugene, OR.
46. **Yamauchi-Takihara, K., M. J. Sole, J. Liew, D. Ing, and C. C. Liew.** 1989. Characterization of human cardiac myosin heavy chain genes. Proc. Natl. Acad. Sci. USA **86:**3504–3508.